Earthquake Research Advances 6 (2026) 100402

Contents lists available at ScienceDirect

Earthquake Research Advances

journal homepage: www.keaipublishing.com/en/journals/earthquake-research-advances

Risk-targeted seismic hazard model for the Philippines

Rhommel Grutas, Jhon Philip Camayang *, Justine Anne Duka, Miguel Antonio Magandi, John Edward Nachor, Jedrek Angelo G. Tupas, Guia Angela C. Agoncillo

Department of Science and Technology – Philippine Institute of Volcanology and Seismology (DOST-PHIVOLCS), Quezon City, 1101, Philippines

ARTICLE INFO

Keywords:
Risk-targeted ground motion
Sensitivity analysis
Seismic hazard mapping
Fragility curves
PSHA

ABSTRACT

The Philippines' current seismic design framework, grounded in outdated uniform hazard approaches, fails to ensure consistent structural safety due to regional variations in seismic risk and structural fragility. This study aims to develop the first risk-targeted seismic hazard maps for the Philippines, adopting the ASCE 7–16 framework and integrating updated probabilistic seismic hazard data from the SHADE Project. Through the application of risk-integral formulations, the annual probability of structural collapse was computed by convolving seismic hazard curves and lognormal fragility functions. A parametric analysis was conducted using varying fragility dispersions ($\beta = 0.6, 0.7, 0.8$) and target collapse probabilities (P_{fail}) to evaluate their effects on risk coefficients (C_R), conditional collapse probabilities, and hazard curve slopes (η) for spectral accelerations at 0.2 s and 1.0 s. Results reveal that higher fragility dispersions and lower collapse targets significantly increase required design motions, particularly in short-period structures. The selected baseline parameters, $\beta = 0.6$ and $P_{fail} = 2 \times 10^{-4}$ (1 % collapse risk in 50 years), yielded consistent collapse probabilities and aligned with international standards. Spatial analyses showed elevated C_R in high-hazard zones such as Western Luzon, Eastern Visayas and Mindanao, while a strong correlation between C_R and η underscores the importance of hazard curve shape in seismic design. All computations assumed rock site conditions, with future work recommended to address site-specific effects.

1. Introduction

Recent advances in earthquake engineering such as improved ground motion models, seismic hazard mapping, and performance-based design have transformed how seismic risks are assessed. These developments highlight the growing need to move beyond traditional approaches toward more risk-targeted methodologies, especially in earthquake-prone countries like the Philippines.

Among the methodologies used for defining seismic design loads, probabilistic seismic hazard analysis (PSHA) remains the most widely adopted approach (Cornell, 1968; McGuire, 2004; Baker et al., 2021). The primary output of PSHA is a hazard curve that defines the relationship between exceedance rate (or return period) and ground motion intensity measures, where selected intensity values are linked to predefined return periods to ensure consistency in seismic loading, following the uniform hazard approach, which applies a consistent annual exceedance frequency across a given region (McGuire, 2004). The Philippines' seismic design criteria outlined in the National Structural Code of the Philippines, 2016 (*NSCP2015*, 2016) are increasingly considered outdated, especially considering significant seismic events that have occurred in recent years. The current framework of the said code is based on the Uniform Building Code (UBC97) (1997) which follows a deterministic approach to seismic hazard determination, relying primarily on source-to-site distances. While this method has

* Corresponding author.
E-mail addresses: rhommel.grutas@phivolcs.dost.gov.ph (R. Grutas), jppcamayang@gmail.com (J.P. Camayang), joduka@up.edu.ph (J.A. Duka), migsmagandi@gmail.com (M.A. Magandi), jednachor@gmail.com (J.E. Nachor), jedrekangelo122199@gmail.com (J.A.G. Tupas), guiaangelaagoncillo@gmail.com (G.A.C. Agoncillo).

Peer review under the responsibility of Editorial Board of Earthquake Research Advances.

Production and Hosting by Elsevier on behalf of KeAi

https://doi.org/10.1016/j.eqrea.2025.100402
Received 30 March 2025; Received in revised form 6 July 2025; Accepted 22 July 2025
2772-4670/© 2025 The Authors. Publishing services by Elsevier B.V. on behalf of KeAi Communications Co. Ltd. This is an open access article under the CC BY license (http://creativecommons.org/licenses/by/4.0/).

Nomenclature

Symbols & Variables

β	Logarithmic standard deviation (fragility dispersion)
η	slope parameter; absolute value of the seismic hazard curve (in log-log scale)
λ	Annual rate of exceedance
C_R	Risk coefficient (ratio of risk-targeted to uniform hazard ground motions)
p (%)	Target probability of collapse (expressed as a percentage)
P_{fail}	Probability of failure or collapse
R^2	coefficient of determination
λ(a)	Mean annual frequency of exceedance for intensity measure level a
F(a)	Fragility function value (probability of collapse given intensity measure level a)

Abbreviations

ASCE	American Society of Civil Engineers
DSHA	Deterministic Seismic Hazard Assessment
EDP	Engineering Demand Parameter
FEMA	Federal Emergency Management Agency
GMPE	Ground Motion Prediction Equation
IM	Intensity Measure
MCE	Maximum Considered Earthquake
MCE_R	Risk-targeted Maximum Considered Earthquake
NEHRP	National Earthquake Hazards Reduction Program
NSCP	National Structural Code of the Philippines
PDF	Probability Density Function
PEM	Philippine Earthquake Model
PSHA	Probabilistic Seismic Hazard Assessment
PHIVOLCS	Philippine Institute of Volcanology and Seismology
RTGM	Risk-Targeted Ground Motion
RTMCE	Risk-Targeted Maximum Considered Earthquake
SA	Spectral Acceleration
SHADE	Seismic Hazard Assessment for Design Earthquake (for the Philippines)
SMTK	Seismic Modeling Tool Kit
T	Period (seconds)
UBC	Uniform Building Code
UHGM	Uniform Hazard Ground Motion

been widely used, it does not fully account for the probabilistic nature of seismic hazards.

In the Philippines, like other countries which utilizes ground motion values in 10 % probability of exceedance in 50 years (equivalent to 475 return period) (*NSCP2015*, 2016), buildings are designed to withstand ground motions with a consistent probability of exceedance. However, it is important to consider the uncertainties in terms of structural collapse capacity, where the seismic design based on uniform hazard ground motion cannot guarantee the uniform risk of structures in different areas (Luco et al., 2007; Spillatura et al., 2023). To solve this, Luco et al. (2007) introduced the risk-targeted approach to obtain seismic design ground motion to get a uniform collapse risk for the regions of USA. At its core, this approach relies on the risk integral, a mathematical fusion of seismic hazard curves and fragility curves, ensuring that structures meet performance expectations without unnecessary overdesign. The risk-targeted approach offers distinct advantages over conventional seismic design methods, including greater transparency, a uniform hazard level within a specific area, and the capability to compare and regulate risk across multiple hazard types, such as earthquakes and wind (Monti et al., 2023).

This study takes the initiative to enhance seismic design methodologies by adopting the ASCE 7–16 framework for developing Risk-Targeted Maximum Considered Earthquake (RTMCE) maps. ASCE 7–16, originally developed in the USA, has been widely adopted in seismically active regions. Countries incorporating a risk-targeted approach include Europe (Silva et al., 2016), New Zealand (Horspool et al., 2021), Iran (Taherian and Kalantari, 2019; Talebi et al., 2021), Malaysia (Arada et al., 2024), Indonesia (Sengara et al., 2020), South Korea (Shin and Kim, 2015), among others, where seismic risk assessment plays a critical role in structural design and safety regulations. Unlike ASCE 7–05 (2005), which primarily utilized deterministic and probabilistic Maximum Considered Earthquake (MCE) ground motion estimates without directly addressing risk uniformity, subsequent updates have progressively introduced risk-based principles. ASCE 7–10 (2013) initiated the shift by recommending ground motion values that more explicitly consider collapse risk. This was further refined in ASCE 7–16 (2017) through the formal adoption of Risk-Targeted Maximum Considered Earthquake (MCE_R) maps, which define seismic hazard levels that achieve a uniform probability of collapse across different locations. The latest edition, ASCE 7–22 (2021), continues this evolution by refining methodologies and data inputs to enhance regional accuracy and reinforce performance-based seismic design goals. This led to the need to advance the generation of Risk-Targeted MCE maps for the Philippines, which has been involved in seismic design codes, such as ASCE 7–16 (2017). Risk-targeted approaches are gaining significant traction in seismic design, and with careful adjustments, they are progressively being incorporated into the next generation of design codes in the Philippines. However, there's a critical gap: how do we determine the right code-compliant seismic risks for different structures? And more importantly, how should risk-targeted design factors be applied effectively? These questions remain largely unexplored. This is precisely why a comprehensive investigation into the development of a 'risk-targeted map' for the Philippines is necessary.

2. Methodology

The annual probability of structural failure, denoted as P_{fail}, beyond a given engineering demand parameter (EDP), can be computed by combining the seismic hazard function with the fragility curve. This process, commonly referred to as risk integration, may be expressed using the following equations (Applied Technology Council, 1978; Luco et al., 2007; Baker et al., 2021):

$$P_{fail} = \int_0^\infty \lambda(a) \cdot \frac{dF(a)}{da} da \tag{1}$$

where $\lambda(a)$ represents the seismic hazard curve, defined as the annual frequency of exceedance for ground motion level a. $F(a)$ denotes the fragility function, usually modeled as a lognormal cumulative distribution, which describes the probability of exceeding a specific damage state given a and $\frac{dF(a)}{da}$ is the fragility probability density function (PDF). This evaluates the failure probability by integrating the product of the hazard function and the fragility density function (i.e., the derivative of the fragility curve). Alternatively, Equa. (2) involves integrating the product of the fragility functions and the derivative od the hazard curve:

$$P_{fail} = -\int_0^\infty F(a) \cdot \frac{d\lambda(a)}{da} da \tag{2}$$

This is particularly useful when the fragility curve is known but the hazard function varies across a dense set of intensity levels. These equations are often referred to as risk integral formulations (McGuire,

2004; Luco et al., 2007), forming the backbone of risk-targeted seismic design.

Through applying this in practice, a relation must first be established between the selected design ground motion intensity and the corresponding fragility curve. When a lognormal model is assumed, the fragility curve is fully characterized by its median capacity and logarithmic standard deviation (β), which together define the curve shape (Porter et al., 2007). A typical choice is to center the fragility curve at the design intensity and calibrate it such that the probability of collapse at that level reflects the structure's intended performance limit (Kennedy, 1999a, 1999b).

This study is limited to the use of spectral accelerations (SA) at 0.2 s and 1.0 s, as provided in the Seismic Hazard Atlas of the Philippines 2024. Therefore, the analysis and generation of risk-targeted ground motion maps were based solely on the available SA values, which are consistent with modern code provisions.

To assess the sensitivity of risk-targeted ground motions (RTGMs) to uncertainty in structural performance, a parametric analysis was conducted by systematically varying the logarithmic standard deviation of fragility ($\beta = 0.6$, 0.7, and 0.8) and target collapse probabilities. These β values reflect different levels of dispersion in structural response due to modeling, material variability, and record-to-record uncertainty. For each β and target collapse probability combination, the corresponding RTGMs, risk coefficients (C_R) and conditional collapse probabilities were computed. This parametric exploration highlights how increasing fragility dispersion leads to higher RTGMs to maintain uniform collapse risk, underscoring the critical influence of β in setting appropriate design ground motions. Thus, the choice of fragility parameters directly affects the resulting design targets, particularly in regions with high hazard variability or limited structural redundancy.

2.1. Seismic hazard model

The Department of Science and Technology – Philippine Institute of Volcanology and Seismology (DOST-PHIVOLCS) has released the Seismic Hazard Atlas for the Design Earthquake of the Philippines (2024) under the SHADE Project. This atlas provides updated Maximum Considered Earthquake (MCE) ground motion maps, integrating probabilistic seismic hazard assessment (PSHA) and deterministic seismic hazard assessment (DSHA) methodologies that will be integrated into the new National Structural Code of the Philippines (NSCP) in collaboration with the Association of Structural Engineers of the Philippines, Inc. (ASEP), ensuring that the latest seismic hazard data informs national engineering design standards for earthquake resilience. Unlike previous models in the Philippines, which relied solely on probabilistic seismic hazard estimates (*PEM*, 2017; Peñarubia et al., 2020), the newly developed MCE maps incorporate both deterministic and probabilistic components, ensuring a more comprehensive seismic design reference. The atlas refines past hazard models by integrating a detailed seismic source model that includes shallow crustal faults, subduction interfaces, and distributed seismicity. Using an earthquake catalog spanning from 1608 to 2022 (containing over 40 375 recorded events), it calculates SA values at 0.2 s and 1.0 s, following ASCE 7-05 standards. The MCE values are determined using a 150 % deterministic factor and a 2 % probability of exceedance in 50 years to reflect long-term hazard considerations. While the study employs advanced modeling techniques for risk-targeted seismic hazard assessments, it is acknowledged that the absence of a centralized empirical damage database in the Philippines limits the ability to directly validate the results using observed structural damage from past major earthquakes, such as 1990 M_S 7.8 Luzon and 2013 M_S 7.2 Bohol events. Currently, there is no national repository that systematically records building-specific damage, collapse data, or structural typologies in sufficient detail to calibrate or validate probabilistic risk estimates. Despite these limitations, the study adopts the risk-integral methodology introduced by Luco et al. (2007), which has been extensively validated in other seismically active countries and incorporated in FEMA P695 (2013) and ASCE 7–16. This provides a scientifically sound basis for approximating collapse probabilities in the Philippine context until more localized empirical data become available. Future efforts should prioritize the development of post-earthquake damage databases and national fragility functions to enable comprehensive calibration and validation of risk-targeted ground motion maps, thereby improving seismic safety planning.

The ground motion prediction equations (GMPEs), presented in Table 1, were applied in the hazard model to account for different seismic source typologies, ensuring consistency between PSHA and DSHA calculations. The selection of GMPEs for the SHADE PSHA model was guided by a rigorous comparative residual analysis. As detailed in Peñarubia et al. (2020), Appendix B, the selection process included 173 waveforms from 18 Philippine earthquakes (M_W 4.9–7.6) with depths less than 50 km and distances under 800 km. Each GMPE was evaluated using OpenQuake's GMPE-SMTK for distances <60 km. The final GMPE weights in SHADE were assigned to reflect both empirical performance and tectonic relevance, with different models used for active shallow crust, subduction interface, and intraslab events. These decisions enhance hazard estimation accuracy by ensuring consistency across both probabilistic and deterministic scenarios.

2.2. Risk-targeted ground motion

The development of a risk-targeted ground motion map requires an iterative procedure. For each site, the hazard curve is first generated using PSHA. Given a target probability of collapse P_{fail} over a specified time horizon (e.g., 1 % in 50 years), the corresponding design intensity is determined by adjusting the spectral acceleration until the risk integral equals the target probability. This iterative adjustment continues until convergence is achieved. Unlike traditional methods based solely on fixed return periods (e.g., SA at 2 475 years), the risk-targeted approach accounts for the full shape of the hazard curve, resulting in design motions adapted to achieve uniform risk across regions (Luco et al., 2007; *FEMA P695*, 2013).

2.3. Standard deviation of structural collapse fragility function

The natural logarithmic standard deviation of structural collapse fragility function, β, measures the uncertainty associated with structural responses under seismic events, often modeled using lognormal distribution functions due to their statistical properties that suit the random nature of seismic loading (Baker, 2015; El-Bahey and Alzeni, 2016). Several studies outline how β informs decisions about structural performance under seismic loads. For instance, Baker (2015) highlights that fragility functions, modeled using lognormal distributions, are standard practice due to their efficiency in conveying the probability of structural collapse against varying ground motion intensities (Baker, 2015).

When using a log-normal function to characterize fragility uncertainty, the standard deviation (β) dictates the curve's steepness that when a higher β, flattens the curve, while a lower β makes it steeper; in an idealized case of zero uncertainty, $\beta = 0$, the fragility curve collapses

Table 1
Ground motion prediction equations (GMPEs) used in modeling.

Source Type	GMPE Model	Weight
Shallow Crustal Faults	ZhaoEtAl2006Asc	0.25
	ChiouYoungs2014	0.25
	BooreEtAl2014LowQ	0.25
	BooreEtAl2014	0.25
Subduction Interface	ParkerEtAl2020SInter	0.33
	ZhaoEtAl2006SInterCascadia	0.34
	AbrahamsonEtAl2015SInter	0.33
Subduction Intraslab	ParkerEtAl2020SSlab	0.33
	AbrahamsonEtAl2015SSlab	0.33
	ZhaoEtAl2006SSlab	0.34

into a vertical line, meaning the probability of structural failure instantly jumps from 0 to 1 once ground motion surpasses the collapse threshold (Baker, 2015; Douglas et al., 2013; Porter et al., 2007; Shinozuka et al., 2000). Other researches indicate that typical values of β for various structural components range from 0.3 to 0.6, depending on factors such as structural type and the level of demand applied (Porter et al., 2007; Bradley, 2010).

While Luco et al. (2007) selected $\beta = 0.8$ based on the collapse assessment of different building systems in the ATC-63 Project (FEMA P-750, 2009; FEMA P695, 2013), ASCE 7–10 (2013) and FEMA P1050 (2015) adopted $\beta = 0.6$. In a similar study, Silva et al. (2016) utilized $\beta = 0.6$ for risk-targeted hazard maps for Europe. Furthermore, Douglas et al. (2013) determined that it is appropriate for France to use $\beta = 0.65$ based on both analytical and statistical analysis. Sengara et al. (2020) in their study revised the β-value from 0.7 to 0.65 for the Indonesian Seismic Building Code.

In the Philippine context, no official set of analytical fragility curves has been established. As a result, this study conducted a parametric analysis using β values of 0.6, 0.7, and 0.8 to assess sensitivity. Based on these results shown in the subsequent analyses and to ensure consistency with international practices, a β value of 0.6 was selected for the final risk-targeted ground motion outputs. This selection reflects a reasonable level of uncertainty for general structural systems while aligning with standards currently recognized in global code development and risk-based design strategies.

2.4. Target collapse probability

A significant percentage of modern design codes (e.g., ASCE 7–16), set a target collapse probability, P_{fail}, of less than 10 % when subjected to the Maximum Considered Earthquake (MCE) shaking hazards (Kim and Han, 2021). Acceptable levels of seismic risk are often defined in terms of both annual and cumulative collapse probabilities over the lifespan of a structure, typically considering a target collapse probability of less than 1% over 50 years, as per FEMA P-750 (Chen et al., 2022).

As noted by Silva et al. (2016), some parameter combinations might be unrealistic due to the strong correlation between β and P_{fail}. For instance, Douglas et al. (2013) highlighted that steeper hazard curves (low β values) are often associated with lower P_{fail}, while Luco et al. (2007) observed that hazard curves with higher probabilities of collapse tend to correspond to larger β values. The acceptable risk collapse in the seismic design code in the USA is defined as 1% in 50 years, equivalent to approximately 2×10^{-4} (*FEMA P695*, 2013). According to FEMA P695 (2013), structures exhibit an average collapse probability of approximately 10 % when subjected to the mapped MCE ground motions. The collapse risk was calculated for general buildings in the Philippines for β values of 0.5, 0.6, 0.7, and 0.8 using Equation (1). Moreover, for this study, the P_{fail} of 10^{-4}, 2×10^{-4} recommended by Luco et al. (2007), 2×10^{-5} and 2×10^{-6} (equivalent to 0.5 %, 1 %, 0.1 % and 0.01 % in 50 years) were considered for the sensitivity analysis. The value $P_{fail} = 2 \times 10^{-4}$, equivalent to a 1 % probability of collapse in 50 years, was adopted as the baseline criterion, in line with recommendations from ASCE 7–16 and FEMA P695 (Luco et al., 2007;FEMA P695, 2013).

2.5. Risk coefficient

Risk coefficient, C_R, is a multiplier applied to the ground motion values (e.g., spectral acceleration) derived from PSHA. It adjusts the hazard values to achieve a target risk level, such as a specific probability of exceedance over a given time period. The risk coefficient ensures that the design ground motions account for uncertainties in the seismic hazard model, including uncertainty in earthquake source characteristics (e.g., location, magnitude and recurrence), variability in GMPEs and epistemic uncertainty in the seismic hazard model. In this study, the risk coefficient is calculated based on Luco et al. (2007):

$$C_R = \frac{\text{Risk Targeted Ground Motion (RTGM)}}{\text{Uniform Hazard Ground Motion (UHGM)}} \quad (3)$$

The risk coefficient adjusts the uniform hazard ground motion UHGM based on the RTGM to align with acceptable risk targets. A risk coefficient value greater than 1 indicates that the RTGM is more conservative than the UHGM, suggesting a higher level of safety or conservatism in the design standards. Conversely, a value less than 1 would indicate a less conservative approach, potentially leading to higher risk levels. This helps ensure that building codes and safety measures are consistent with the desired level of risk management.

3. Results and discussions

This study presents the first risk-targeted ground motion maps for the Philippines, utilizing a methodology aligned with ASCE 7–16. Through integrating PSHA-based hazard curves with fragility functions through risk integral formulations, the research aimed to identify spatially consistent design intensities that correspond to a target probability of collapse. The resulting risk coefficients and collapse probabilities provide valuable understanding of how ground motion uncertainties and regional seismicity influence seismic design.

3.1. Relationships of P_{fail} and C_R

The relationship between the C_R and conditional probability of collapse across different fragility dispersions (β), ground motion periods (SA at T = 0.2 s and 1.0 s), and hazard levels, is illustrated in Fig. 1. Results illustrate the sensitivity of C_R to varying collapse probabilities and fragility dispersions for both SA (0.2 s and 1.0 s) in the Philippines. Across all evaluated scenarios, an increase in β consistently yields higher C_R, indicating a greater adjustment is needed to achieve target risk levels under higher uncertainty. As the target collapse probability, P_{fail}, becomes more conservative (lower), the required C_R significantly increases, particularly evident in the short-period, SA (0.2 s), case. This reflects the sharper ground motion scaling to compensate for stricter performance objectives (see Fig. 2).

In both periods, the trendlines remain relatively stable across the range of collapse probabilities p (%), suggesting that the risk coefficient is dominated by β and P_{fail} rather than the collapse probability itself. However, the amplification is more prominent in SA (0.2 s), indicating that short-period structures are more sensitive to risk adjustments, particularly at lower failure probabilities. These results highlight the importance of period- and fragility-specific calibration in risk-targeted ground motion design, particularly in regions such as the Philippines, where hazard levels and uncertainties vary spatially.

Moreover, Table 2 presents the average conditional collapse probabilities (in %) calculated using Equa. (2). As β increases from 0.6 to 0.8, the average p (%) also increases, reflecting greater structural uncertainty and, consequently, higher collapse probabilities. Across varying P_{fail} levels, the average p (%) remains relatively stable, indicating that the risk-targeted design method successfully maintains consistent collapse probabilities regardless of the risk target. Furthermore, results show that C_R they increase with both β and more conservative P_{fail} values. For lower β, C_R is relatively insensitive to changes in p (%), whereas higher β values result in steeper C_R-p (%) trends, highlighting the amplifying role of fragility dispersion in risk-targeted ground motion estimates. Additionally, SA (0.2 s) consistently yields slightly higher p (%) values than SA (1.0 s), suggesting that short-period structures are generally more vulnerable to collapse under seismic loading.

Additionally, Fig. 2 presents the spatial distribution of the C_R across the Philippines for SA(0.2 s) and SA(1.0 s), considering increasing values of fragility uncertainty ($\beta = 0.6$, 0.7, and 0.8) and a target annual probability of collapse $P_{fail} = 2 \times 10^{-4}$ (equivalent to 1% in 50 years), which aligns with widely accepted design standards such as ASCE 7–16

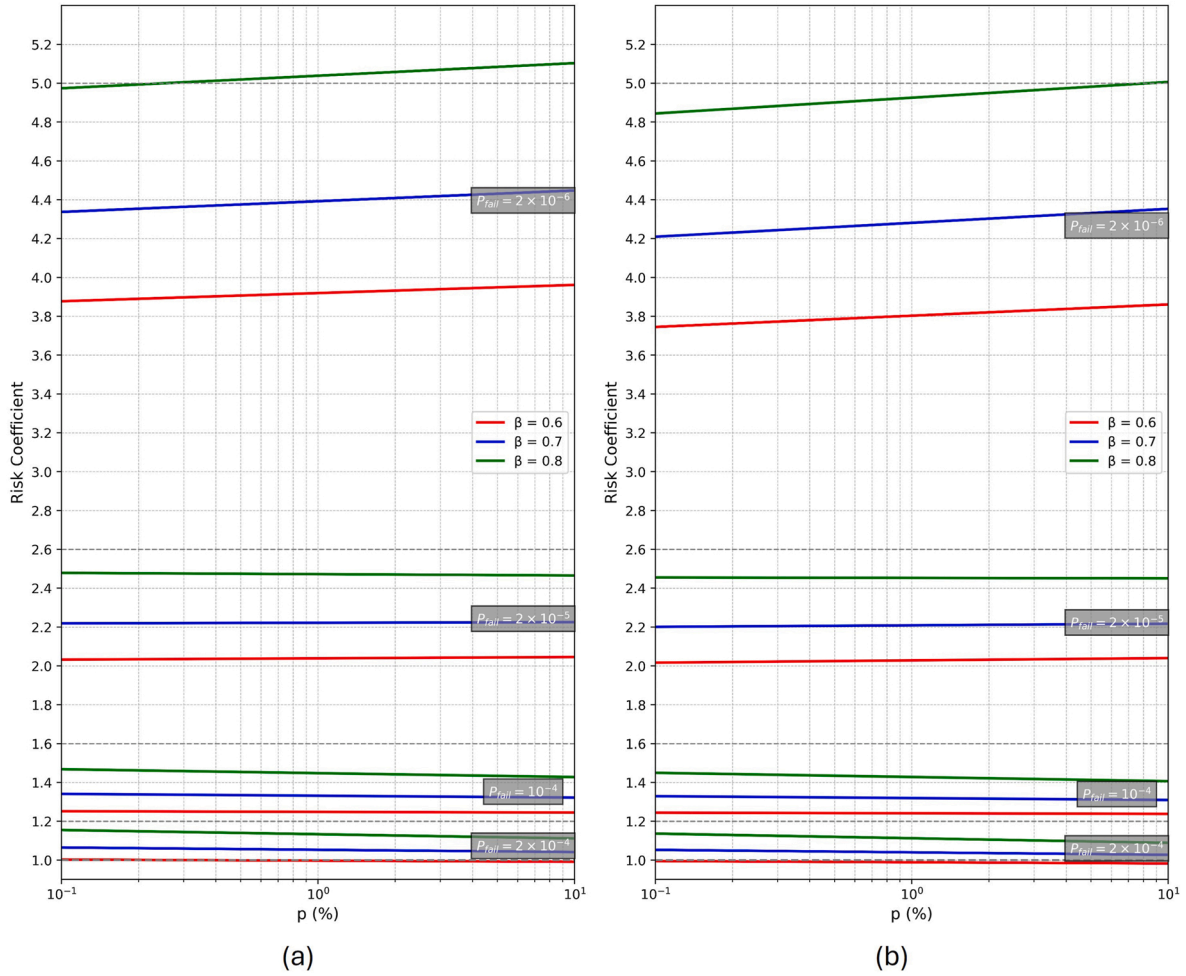

Fig. 1. Relation between the C_R and p (%) at (a) SA (0.2 s) and (b) SA (1.0 s) for the Philippines when $P_{fail} = 10^{-4}$, 2×10^{-4}, 2×10^{-5} and 2×10^{-6} across different lognormal dispersions ($\beta = 0.6$, 0.7 and 0.8). subtle pronounced modest.

and FEMA P695. Results indicate that C_R increases significantly with higher β, demonstrating that greater uncertainty in collapse capacity necessitates more conservative design motions. High-risk areas, particularly along the Philippine Fault Zone, exhibit the largest C_R values, especially for $\beta = 0.8$, signifying amplified seismic demand under elevated structural fragility. Additionally, the C_R values are generally higher in SA(0.2 s) compared to SA(1.0 s), emphasizing the heightened vulnerability of short-period structures. The use of $P_{fail} = 2 \times 10^{-4}$ as a baseline reflects an appropriate safety threshold, aiming for a uniform 1 % probability of collapse in 50 years, which is considered acceptable for standard-risk structures in seismic design frameworks.

To support the spatial interpretation of regional risk variations, Table 3 presents the minimum, maximum, and mean risk coefficient values C_R across Philippine regions for both SA(0.2 s) and SA(1.0 s) periods. These values quantitatively reinforce the observed spatial disparities in seismic risk across the country, offering useful input for region-specific seismic design.

3.2. Relationship between the hazard curve and the C_R

This study investigates the influence of the seismic hazard curve on C_R. The slope parameter, referred to as η, is defined as the absolute value of the derivative of the seismic hazard curve (in log-log scale). It captures how rapidly ground motion intensity increases as the probability of exceedance decreases, which is defined as:

$$\eta = \left| \frac{d \log (\lambda)}{d \log (IM)} \right| \tag{4}$$

where λ is the annual rate of exceedance and IM is the ground motion intensity measure (e.g., spectral acceleration). This formulation is consistent with the hazard slope metrics used in simplified risk models and performance-based frameworks (e.g., Crowley et al., 2009; Vamvatsikos, 2013; Cito and Iervolino, 2024). To evaluate the influence of the hazard curve's steepness on the seismic design ground motion, this study explored the correlation between the computed C_R and the log-log slope of the seismic hazard curve, η. Fig. 3 illustrates the linear regression results for both short-period spectral acceleration (SA (0.2 s)) and long-period spectral acceleration (SA (1.0 s)), under varying values of the logarithmic standard deviation of fragility $\beta = 0.6$, 0.7, 0.8. The results show a strong and consistent linear relationship between C_R and η across all cases, with coefficients of determination (R^2) exceeding 0.93 in each subplot. This confirms that the shape of the hazard curve, captured by η, is correlated with the adjustment from UHGM to RTGM. As the slope η increases, which indicates a steeper hazard curve, the risk coefficient also increases, reflecting the need for greater conservatism in seismic design to achieve uniform collapse probabilities. Moreover, the linear regression slopes increase with higher values of β, indicating that fragility dispersion amplifies the sensitivity of risk coefficients to the slope of the hazard curve. This effect is particularly evident in both SA (0.2 s) and SA (1.0 s) cases, where $\beta = 0.8$ consistently yields the highest

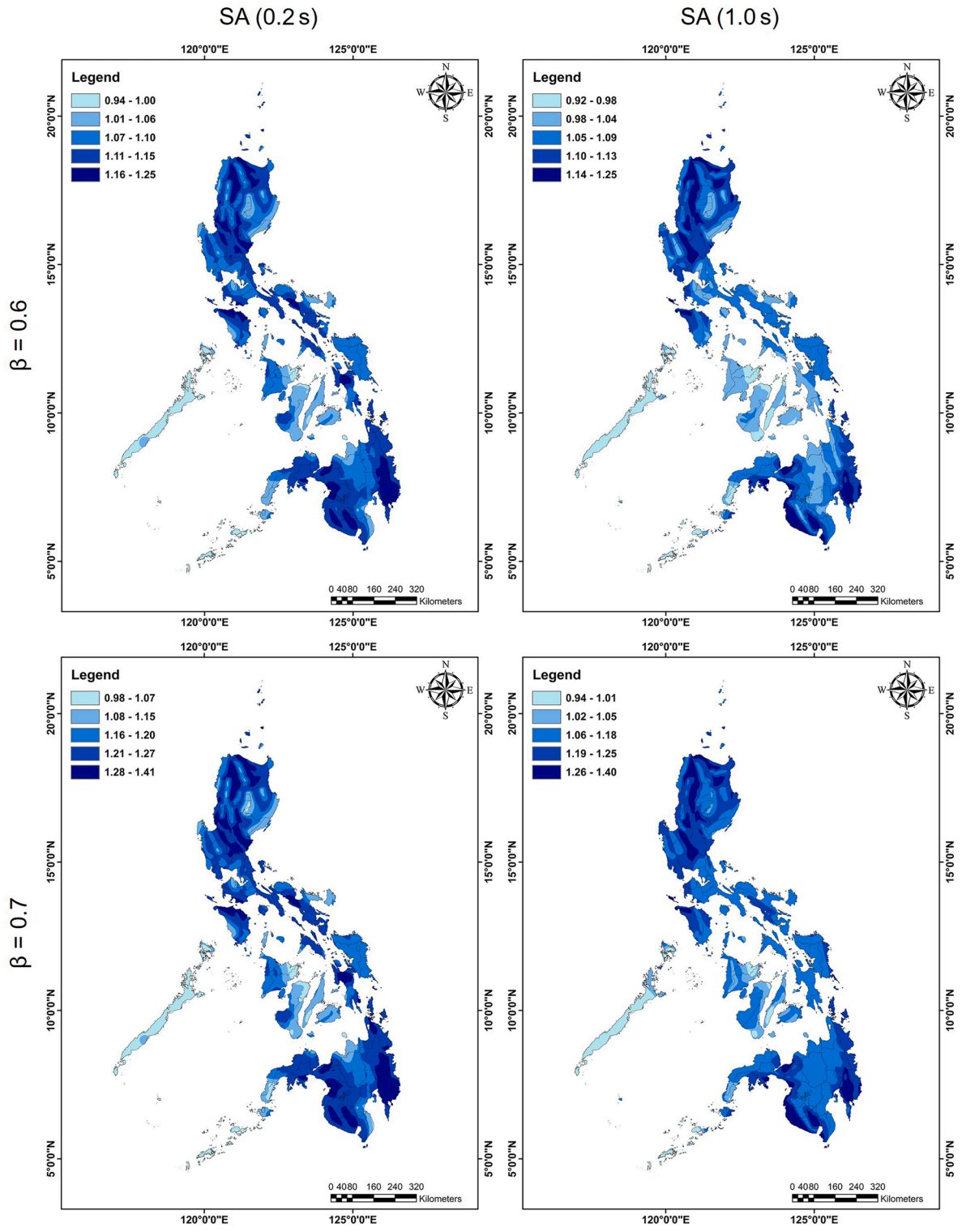

Fig. 2. Risk coefficient map in the Philippines for SA (0.2 s) and SA (1.0 s), assuming $\beta = 0.6$, 0.7, 0.8 and $P_{fail} = 2 \times 10^{-4}$

regression slopes, indicating that uncertainty in structural capacity amplifies the impact of hazard curve steepness on design motion adjustments. By integrating η into the calibration of risk coefficients, this study presents an effective framework for developing more rational and location-sensitive seismic risk management strategies.

3.3. Risk-targeted maps for the Philippines

The seismic risk maps are plotted in Fig. 4 with risk of collapse, $P_{fail} = 2 \times 10^{-4}$ for $\beta = 0.6$. The annual risk of collapse varies across different regions in each plot. Thus, the need for the generation of risk-targeted seismic design maps for the Philippines becomes evident.

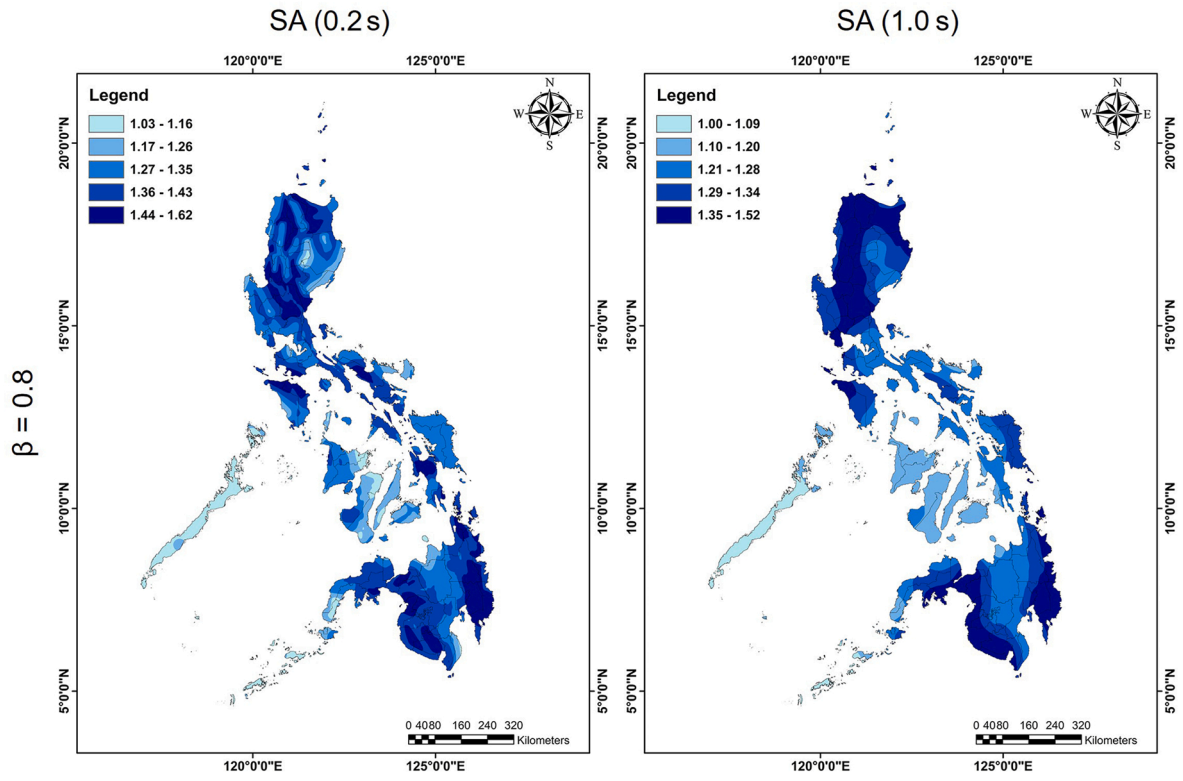

Fig. 2. (*continued*).

Table 2
Average conditional probability of collapse p (%) across all sites, for different combinations of target collapse probabilities (0.5%, 1%, 0.1% and 0.01%), spectral accelerations (at T = 0.2 s and 1.0 s) and fragility curve dispersion (β).

β	$P_{fail} = 0.005$		$P_{fail} = 0.01$		$P_{fail} = 0.001$		$P_{fail} = 0.0001$	
	SA (0.2 s)	**SA (1.0 s)**	**SA (0.2 s)**	**SA (1.0 s)**	**SA (0.2 s)**	**SA (1.0 s)**	**SA (0.2 s)**	**SA (1.0 s)**
0.6	0.3697	0.3457	0.3692	0.3452	0.3708	0.3469	0.3715	0.3477
0.7	0.3727	0.3496	0.3722	0.3491	0.3739	0.3508	0.3746	0.3515
0.8	0.3757	0.3536	0.3753	0.3531	0.3769	0.3548	0.3776	0.3555

Table 3
Summary of C_R's per Philippine region for SA(0.2 s) and SA(1.0) periods, illustrating regional variability in seismic demand.

Region	SA(0.2 s)			SA(1.0 s)		
	Min.	Max.	Mean	Min.	Max.	Mean
LUZON						
National Capital Region (NCR)	1.04594	1.07784	1.05527	1.00409	1.07510	1.01624
CAR - Cordillera Administrative Region	1.00433	1.24585	1.11863	0.99074	1.23501	1.10417
I - Ilocos Region	1.03128	1.24559	1.11166	1.01619	1.24139	1.10286
II - Cagayan Valley	1.00221	1.19163	1.10354	0.98681	1.16745	1.09327
III - Central Luzon	1.01654	1.17542	1.11054	0.98428	1.16677	1.09248
IV-A - CALABARZON	1.03726	1.16586	1.10303	0.99844	1.13396	1.05788
IV-B - MIMAROPA	0.94000	1.19253	1.03208	0.94000	1.14373	1.00911
V - Bicol Region	0.98884	1.17292	1.10050	0.95632	1.09315	1.05456
VISAYAS						
VI - Western Visayas	0.97387	1.14857	1.06074	0.95100	1.05910	0.99027
Negros Island Region (NIR)	0.98300	1.12805	1.05011	0.95665	1.06113	1.00537
VII - Central Visayas	0.98721	1.10279	1.03878	0.94022	1.03250	0.98942
VIII - Eastern Visayas	1.03381	1.17025	1.09354	0.99098	1.11365	1.05402
MINDANAO						
IX - Zamboanga Peninsula	1.00196	1.15907	1.09096	0.96442	1.14934	1.05982
X - Northern Mindanao	0.97999	1.18759	1.08614	0.97124	1.17337	1.05358
XI - Davao Region	0.99168	1.22370	1.12460	0.99963	1.18484	1.09119
XII - SOCCSKSARGEN	1.06024	1.18294	1.13292	1.00798	1.20566	1.10013
XIII - Caraga	1.06743	1.19535	1.12754	1.00216	1.14312	1.07430
Bangsamoro Autonomous Region In Muslim Mindanao (BARMM)	0.95854	1.19769	1.09858	1.07430	1.19705	1.06588

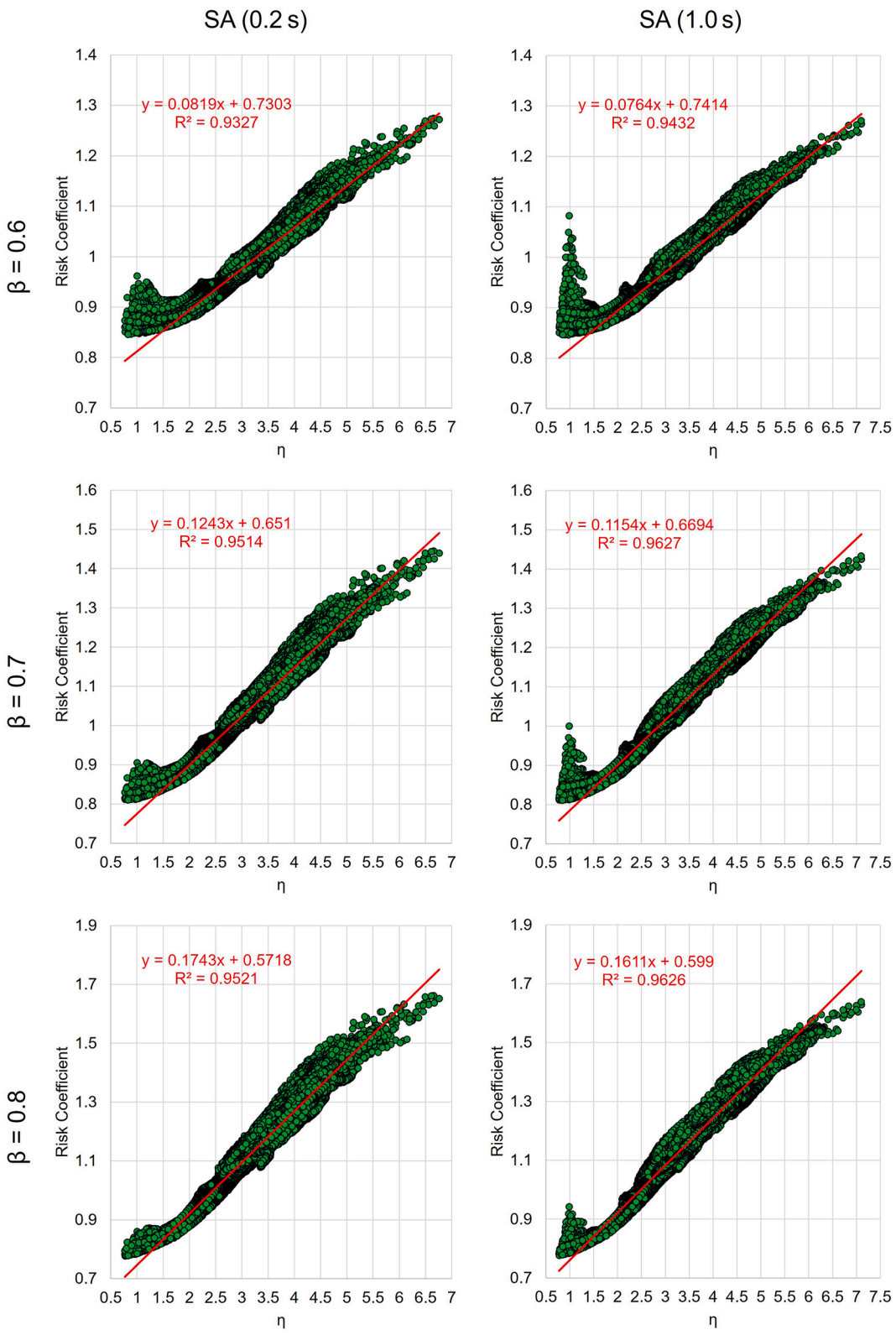

Fig. 3. Relationship between the risk coefficient C_R and the slope of the seismic hazard curve η, for varying fragility dispersions β from 0.6 to 0.8.

As show in Table 3, higher C_R values are predominantly observed in seismically active regions such as the western margins of Luzon, the Leyte-Samar area (part of Visayas), and parts of Mindanao, reflecting the need for amplified ground motion levels to meet uniform collapse risk targets as illustrated in Fig. 5. Notably, the C_R values are generally greater for SA (0.2 s), indicating that short-period structures require more conservative adjustments to meet target risk levels compared to longer-period systems. This spatial variation highlights the influence of local hazard curve shapes on seismic design and underscores the value of risk-targeted approaches in achieving geographically consistent performance objectives.

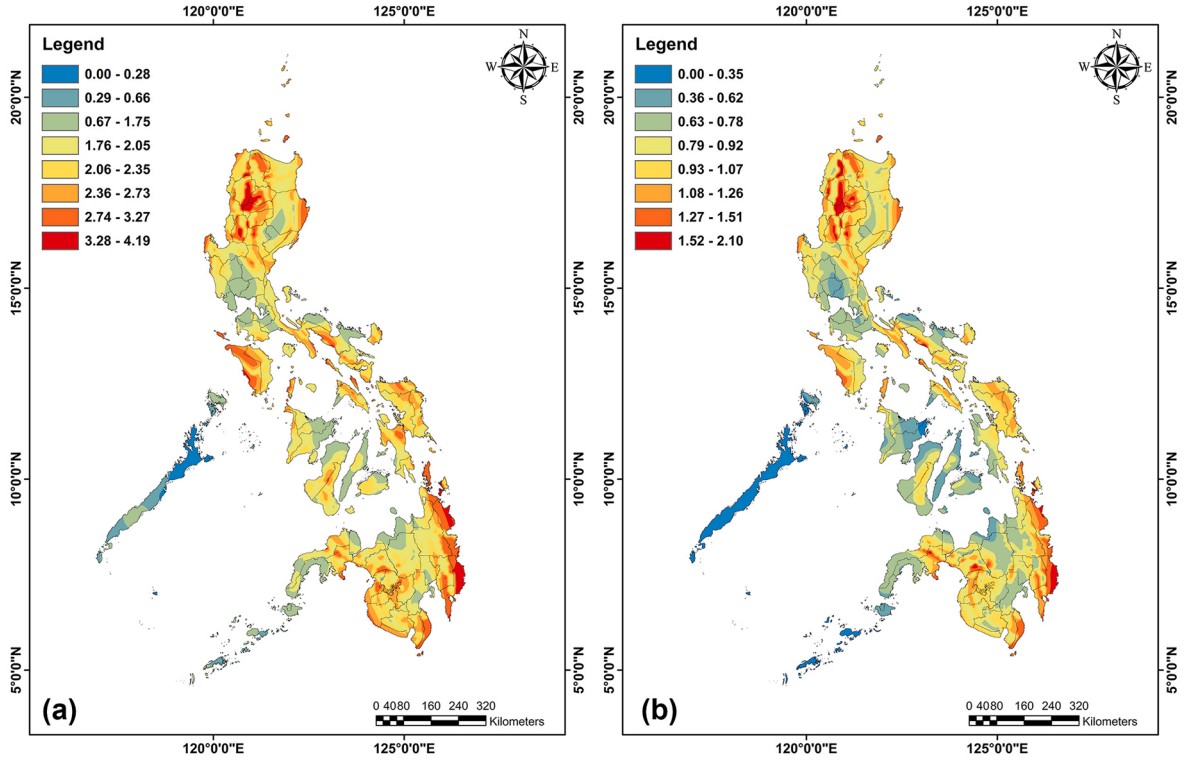

Fig. 4. Risk-targeted maximum considered earthquake ground motion maps for the Philippines at SA (0.2 s) and SA (1.0 s) for fragility dispersion, $\beta = 0.6$.

The risk-targeted MCE maps produced in this study provide an improved framework for seismic design in the Philippines. Unlike traditional return-period-based methods, these maps ensure that buildings are designed to meet consistent collapse risk targets, irrespective of location. Given the Philippines' complex tectonic setting, applying uniform collapse probability criteria is critical for achieving equitable safety standards.

While this study focuses on spectral accelerations at 0.2 s and 1.0 s, which correspond to the typical response periods for buildings, it is acknowledged that this scope does not fully represent the seismic demands on taller structures. Long-period buildings are more sensitive to ground motions with spectral periods around 2.0 s or greater. The current emphasis provides a practical baseline for most building classes; however, future risk-targeted mapping efforts should be expanded to include additional spectral periods (e.g., 2.0 s) to ensure comprehensive coverage across a broader range of structural typologies. Expanding the framework to incorporate transitional and long-period spectral accelerations is recommended. This will enhance the applicability of the framework for diverse engineering applications and further align with performance-based seismic design goals for tall buildings in urban areas.

The resulting risk-targeted ground motion values presented in this study are derived under the assumption of rock site conditions (Site Class B/C), consistent with regional PSHA methodologies. While this allows for standardized comparisons across the country, it is important to interpret these results within the context of local geologic diversity. In particular, urban regions like Metro Manila, which are underlain by soft soil deposits, may experience significantly higher ground motion amplification than what is reflected in the current maps. This suggests that the presented risk coefficients (C_R) may underestimate seismic demands in such areas. Although the current analysis provides a reliable national baseline, extending this framework to include site amplification factors would enhance the resolution of seismic risk assessments.

While this study focuses on the technical development of risk-targeted ground motion maps, recent initiatives of the DOST-PHIVOLCS, such as the Iloilo City Earthquake Model (*ICEM*, 2023) and Butuan City Earthquake Model (*BCEM*, 2025), highlight how earthquake risk outputs are being operationalized in the said Philippine cities. These are currently the only documented studies that demonstrate the localized applications of seismic risk information. In particular, the loss maps generated from these models were developed to estimate expected building damage and economic loss at the Barangay level, serving as tools for urban land-use planning, emergency preparedness and prioritization of retrofitting investments. These applications underscore the broader economic and social relevance of risk-targeted seismic design, showing its potential not only in structural engineering but also in guiding policy, disaster mitigation programs and resilience-oriented development in at-risk communities.

4. Conclusion and recommendations

This study presents the first development of risk-targeted ground motion maps for the Philippines, using a methodology based on the ASCE 7–16 framework and supported by the most recent PSHA results from the SHADE Project. Through risk-integral formulations, the annual probability of collapse (P_{fail}) was assessed by combining probabilistic seismic hazard curves and lognormal fragility functions. A parametric analysis was carried out to explore the sensitivity of design ground motions to variations in fragility dispersion (logarithmic standard deviation, β) and target collapse probabilities. Risk coefficients (C_R), conditional collapse probabilities (p(%)), and hazard curve slope parameters (η) were computed for ground motion periods SA(0.2 s) and SA (1.0 s) across the Philippines.

Findings confirm that higher fragility dispersions (β) and more conservative target collapse probabilities lead to significantly increased C_R values, indicating more conservative design ground motions. Short-period structures (SA at 0.2 s) showed heightened sensitivity to risk adjustments, particularly under elevated uncertainty. Spatial variations in C_R were closely aligned with known high-hazard regions, including areas along the Philippine Fault Zone, Eastern Luzon, Leyte-Samar, and parts of Mindanao. A strong linear relationship between C_R and hazard

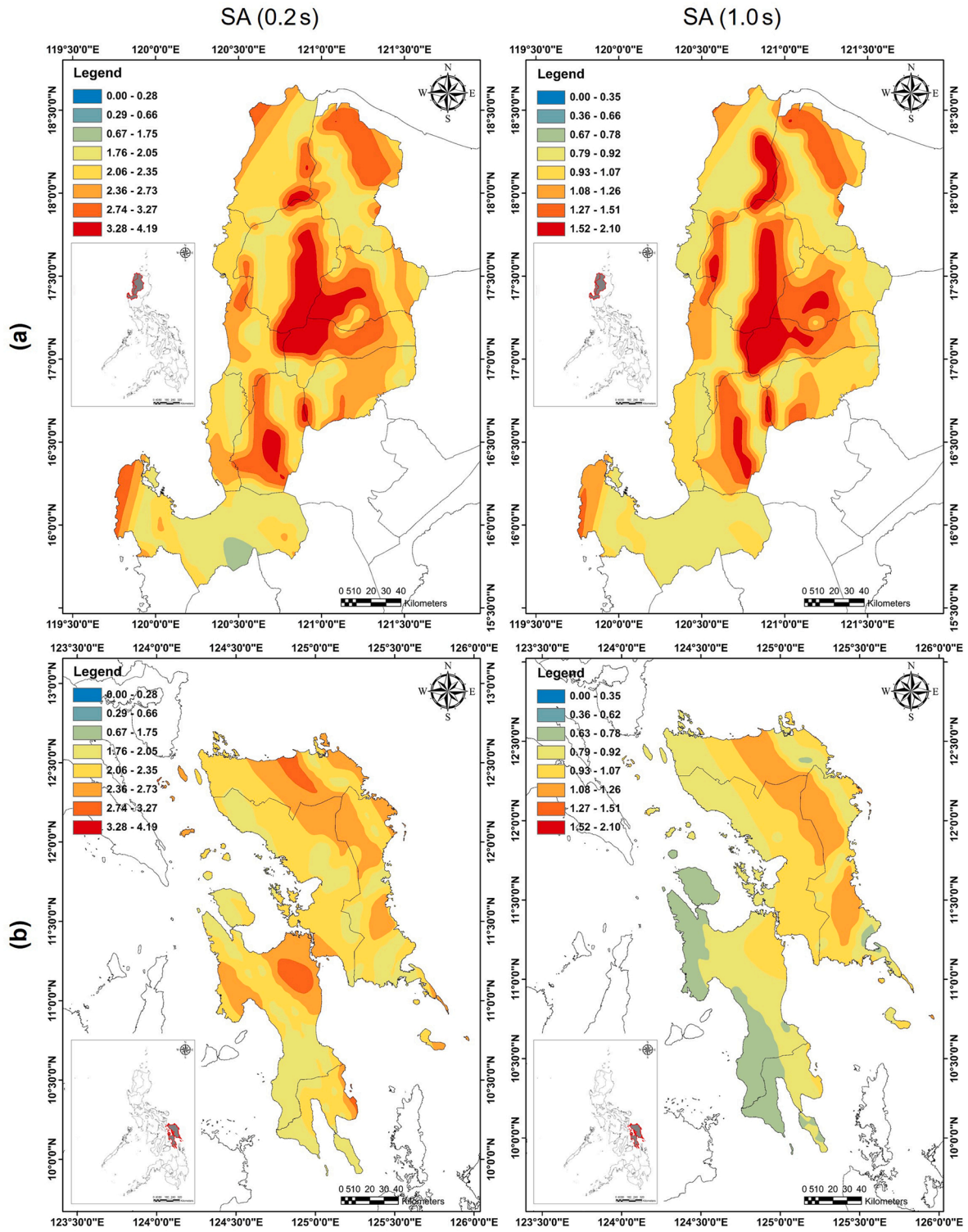

Fig. 5. RTMCE spatial distribution of elevated risk coefficients C_R for SA(0.2 s) and SA(1.0 s) across (a) Luzon, (b) Visayas, and (c–d) Mindanao assuming $\beta = 0.6$ and $P_{fail} = 2 \times 10^{-4}$

curve slope η further emphasizes the importance of accounting for local hazard characteristics in seismic design. The study adopted $\beta = 0.6$ and $P_{fail} = 2 \times 10^{-4}$ (equivalent to a 1 % probability of collapse in 50 years) as final parameters for the generating the risk-targeted MCE maps. These values reflect international standards (e.g., FEMA P695, ASCE 7–16) and have been found to yield stable and consistent collapse probabilities across varying hazard and structural scenarios. The results reinforce the importance of using risk-consistent metrics for seismic design, ensuring uniform safety levels across geographic regions.

Furthermore, the current analysis is limited to spectral periods, 0.2 s and 1.0 s, which primarily capture the seismic demands on structures. To extend the applicability of risk-targeted ground motion maps to tall buildings and long-period infrastructure, future studies should include additional periods (e.g., 2.0s) in the spectral analysis. This would

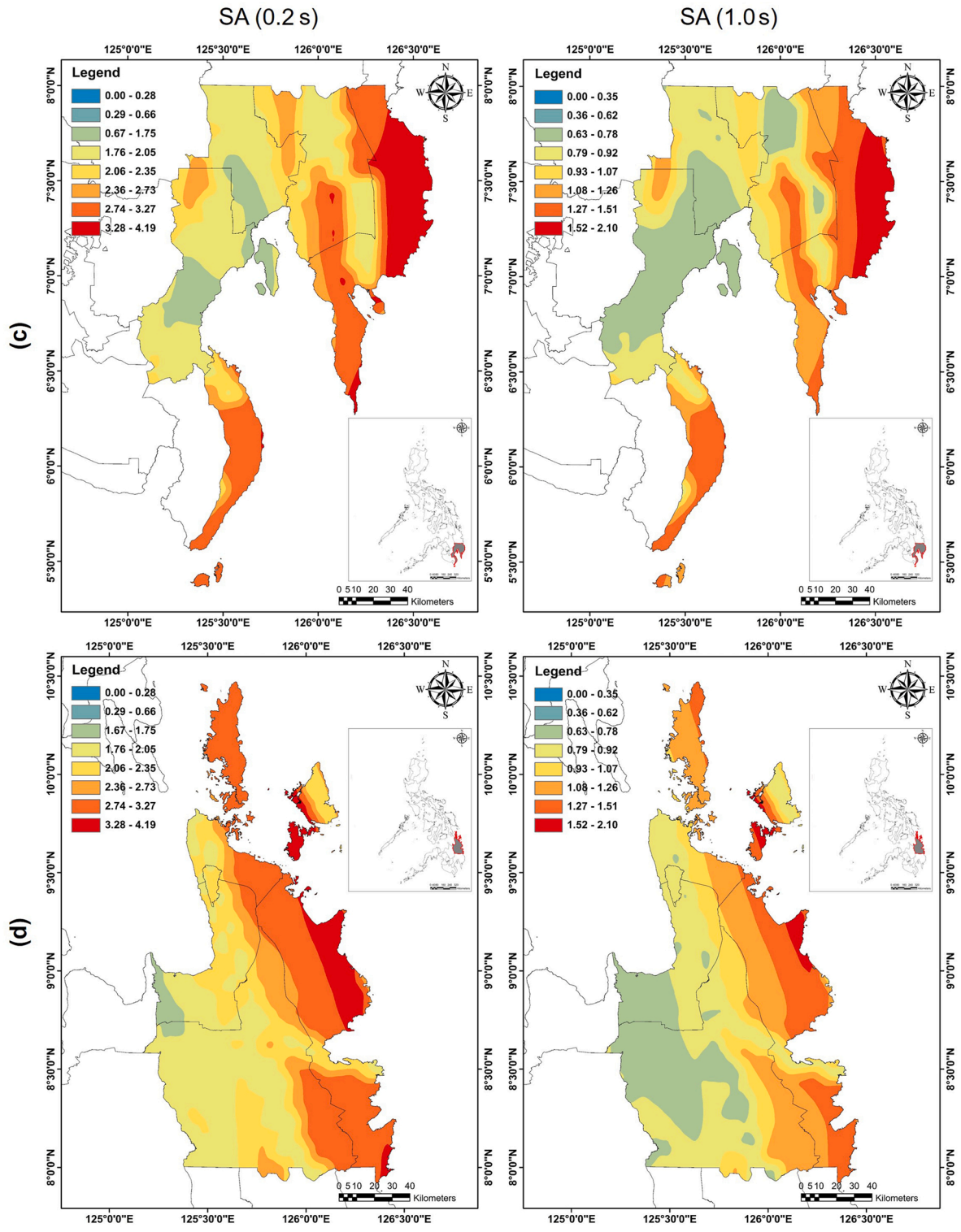

Fig. 5. (*continued*).

support a more inclusive framework for performance-based design across diverse structural typologies. All calculations in this study were performed assuming rock site conditions, which are commonly used as reference conditions in PSHA and ground motion modeling. While this standard approach ensures consistency, it does not account for site-specific amplification effects. This limitation is fundamental in the Philippine context, where diverse geologic and geotechnical conditions (e.g., soft soils, liquefiable deposits) can significantly amplify seismic demand. However, the absence of a nationwide, published site amplification database remains a key constraint in refining hazard assessment. These localized effects may lead to an underestimation of seismic risk in certain areas. Future studies should therefore incorporate site amplification models or conduct site-specific response analyses to enhance the resolution and applicability of risk-targeted ground motion maps. For practical implementation, integrating these refined ground motions into future seismic code updates is crucial to ensure uniform safety standards

nationwide. To advance seismic resilience in the Philippines, it is recommended to integrate risk-targeted ground motions into future seismic code updates, leading the adoption to ensure uniform safety nationwide. Developing national fragility curves for the local building stock is essential to improve the accuracy of risk-targeted assessments.

CRediT authorship contribution statement

Rhommel Grutas: Writing – review & editing, Supervision, Project administration, Methodology, Funding acquisition, Conceptualization. **Jhon Philip Camayang:** Writing – review & editing, Writing – original draft, Visualization, Validation, Resources, Project administration, Methodology, Investigation, Formal analysis, Data curation, Conceptualization. **Justine Anne Duka:** Writing – review & editing, Validation, Investigation. **Miguel Antonio Magandi:** Writing – review & editing, Validation, Resources, Project administration, Methodology, Investigation. **John Edward Nachor:** Writing – review & editing, Validation, Resources, Methodology, Investigation. **Jedrek Angelo G. Tupas:** Visualization, Validation, Resources, Methodology, Investigation, Formal analysis. **Guia Angela C. Agoncillo:** Writing – review & editing, Resources, Investigation.

Declaration of competing interest

The authors declare that they have no known competing financial interests or personal relationships that could have appeared to influence the work reported in this paper.

Author agreement and acknowledgments

The authors express their gratitude to the Department of Science and Technology - Philippine Institute of Volcanology and Seismology (DOST-PHIVOLCS), under the leadership of Dr. Teresito C. Bacolcol, Dr. Ma. Mylene M. Villegas, Sir Ishmael C. Narag and Dr. Winchelle Ian G. Sevilla, for serving as the implementing agency for this research. Acknowledgment is also extended to the Department of Science and Technology (DOST) as a funding agency for the SHADE Project and Department of Science and Technology - Philippine Council for Industry, Energy, and Emerging Technology Research and Development (DOST-PCIEERD) for their support as the monitoring agency. The contributions of Project SHADE staff, including Nicole Ann Bersabe, Montgomery van Brussel Toft, Rizza Micaela Padre, Koreen Dorado, and Louise Anthony Alparaque are sincerely appreciated–their commitment and teamwork were instrumental in addressing the complex challenges of seismic hazard assessment and ensuring the timely completion of this study.

References

Applied Technology Council, 1978. Tentative Provisions for the Development of Seismic Regulations for Buildings: a Cooperative Effort with the Design Professions, Building Code Interests and the Research Community (No. NBS SP 510; 0 Ed., P. NBS SP 510). National Bureau of Standards. https://doi.org/10.6028/NBS.SP.510.

Arada, A.H., Majid, T.A., Choong, K.K., 2024. A step toward developing risk-targeted seismic design maps for Malaysia. Part 1: a representative exposure model. Arabian J. Sci. Eng. https://doi.org/10.1007/s13369-024-09822-9.

Baker, J.W., 2015. Efficient analytical fragility function fitting using dynamic structural analysis. Earthq. Spectra 31 (1), 579–599. https://doi.org/10.1193/021113EQS025M.

Baker, J.W., Bradley, B., Stafford, P., 2021. Seismic Hazard and Risk Analysis, first ed. Cambridge University Press. https://doi.org/10.1017/9781108425056.

Bradley, B.A., 2010. Epistemic uncertainties in component fragility functions. Earthq. Spectra 26 (1), 41–62. https://doi.org/10.1193/1.3281681.

Butuan City Earthquake Model: Event-Based Probabilistic Seismic Risk Assessment, 2025. (with Philippine Institute of Volcanology and Seismology) 1. ISBN. https://www.phivolcs.dost.gov.ph/index.php/publications/books/seismic-hazard-and-ground-motion-atlases.

Chen, J., Wang, W., Fang, C., 2022. Seismic collapse capacity and dispersion spectra for self-centering braced frames considering uncertainty propagation. Earthq. Eng. Struct. Dynam. 51 (14), 3367–3392. https://doi.org/10.1002/eqe.3727.

Cito, P., Iervolino, I., 2024. Drivers to seismic hazard curve slope. Earthq. Eng. Struct. Dynam. 53 (15), 4497–4510. https://doi.org/10.1002/eqe.4226.

Cornell, C.A., 1968. Engineering seismic risk analysis. Bull. Seismol. Soc. Am. 58 (5), 1583–1606. https://doi.org/10.1785/BSSA0580051583.

Crowley, H., Colombi, M., Borzi, B., Faravelli, M., Onida, M., Lopez, M., Polli, D., Meroni, F., Pinho, R., 2009. A comparison of seismic risk maps for Italy. Bull. Earthq. Eng. 7 (1), 149–180. https://doi.org/10.1007/s10518-008-9100-7.

Douglas, J., Ulrich, T., Negulescu, C., 2013. Risk-targeted seismic design maps for mainland France. Nat. Hazards 65 (3), 1999–2013. https://doi.org/10.1007/s11069-012-0460-6.

El-Bahey, S., Alzeni, Y., 2016. Effect of soil structure interaction on the seismic fragility of a nuclear reactor building. Volume 1: Operations and Maintenance, Aging Management and Plant Upgrades; Nuclear Fuel, Fuel Cycle, Reactor Physics and Transport Theory; Plant Systems, Structures, Components and Materials; I&C, Digital Controls, and Influence of Human Factors. https://doi.org/10.1115/ICONE24-60714. V001T03A021.

Horspool, N., Hulsey, A., Elwood, K., Gerstenberger, M., 2021. Risk Targeted Hazard Spectra for Seismic Design in New Zealand.

Iloilo city earthquake model: event-based probabilistic seismic risk assessment (vol. 1) (with Philippine institute of volcanology and seismology), Department of Science and Technology - Philippine Institute of Volcanology and Seismology (DOST - PHIVOLCS), 2023. https://www.phivolcs.dost.gov.ph/index.php/publications/books/seismic-hazard-and-ground-motion-atlases.

Kennedy, R.P., 1999a. Overview of methods for seismic PRA and margins analysis. Reliab. Eng. Syst. Saf. 65 (2), 171–179.

Kennedy, R.P., 1999b. Risk based seismic design criteria. Nucl. Eng. Des. 192 (2–3), 117–135. https://doi.org/10.1016/S0029-5493(99)00102-8.

Kim, T., Han, S.W., 2021. Seismic collapse performance of steel special moment frames designed using different analysis methods. Earthq. Spectra 37 (2), 988–1012. https://doi.org/10.1177/8755293020970969.

Luco, N., Ellingwood, B.R., Hamburger, R.O., Hooper, J.D., Kimball, J.K., Kircher, C.A., 2007. Risk-targeted versus current seismic design maps for the conterminous United States. SEAOC 2007 Convention Proceedings 13.

McGuire, R.K., 2004. Seismic Hazard and Risk Analysis. Earthquake Engineering Research Institute. https://books.google.com.ph/books?id=ZUVCAQAAIAAJ.

Monti, G., Demartino, C., Gardoni, P., 2023. Towards risk-targeted seismic hazard models for Europe. Sci. Rep. 13 (1), 10717. https://doi.org/10.1038/s41598-023-36947-y.

National Structural Code of the Philippines 2015, 2016. Association of Structural Engineers of the Philippines, Inc (Seventh edition, Vol. 1) (with Association of Structural Engineers of the Philippines (ASEP)).

Peñarubia, H.C., Johnson, K.L., Styron, R.H., Bacolcol, T.C., Sevilla, W.I.G., Perez, J.S., Bonita, J.D., Narag, I.C., Solidum, R.U., Pagani, M.M., Allen, T.I., 2020. Probabilistic seismic hazard analysis model for the Philippines. Earthq. Spectra 36 (1_Suppl. l), 44–68. https://doi.org/10.1177/8755293019900521.

Philippine Earthquake Model (PEM): a Probabilistic Seismic Hazard Assessment of the Philippines and of Metro Manila (With Philippine Institute of Volcanology and Seismology (DOST-PHIVOLCS)), 2017. Department of Science and Technology - Philippine Institute of Volcanology and Seismology.

Porter, K., Kennedy, R., Bachman, R., 2007. Creating fragility functions for performance-based earthquake engineering. Earthq. Spectra 23 (2), 471–489. https://doi.org/10.1193/1.2720892.

Seismic hazard atlas for the design earthquake of the Philippines (with Philippine institute of volcanology and seismology (DOST - phivolcs)). Department of Science and Technology - Philippine Institute of Volcanology and Seismology (DOST - PHIVOLCS), 2024.

Sengara, I.W., Irsyam, M., Sidi, I.D., Mulia, A., Asrurifak, M., Hutabarat, D., Partono, W., 2020. New 2019 risk-targeted ground motions for spectral design criteria in Indonesian seismic building code. E3S Web of Conferences 156, 03010. https://doi.org/10.1051/e3sconf/202015603010.

Shin, D.H., Kim, H.-J., 2015. Domestic seismic design maps based on risk-targeted Maximum- considered earthquakes. Journal of the Earthquake Engineering Society of Korea 19 (3), 93–102. https://doi.org/10.5000/EESK.2015.19.3.093.

Shinozuka, M., Feng, M.Q., Lee, J., Naganuma, T., 2000. Statistical analysis of fragility curves. J. Eng. Mech. 126 (12), 1224–1231. https://doi.org/10.1061/(ASCE)0733-9399(2000)126:12(1224.

Silva, V., Crowley, H., Bazzurro, P., 2016. Exploring risk-targeted hazard maps for Europe. Earthq. Spectra 32 (2). https://doi.org/10.1193/112514eqs198m. Article 2.

Spillatura, A., Vamvatsikos, D., Kohrangi, M., Bazzurro, P., 2023. Harmonizing seismic performance via risk targeted spectra: state of the art, dependencies, and implementation proposals. Earthq. Eng. Struct. Dynam. 52 (13), 4277–4299. https://doi.org/10.1002/eqe.3941.

Taherian, A.R., Kalantari, A., 2019. Risk-targeted seismic design maps for Iran. J. Seismol. 23 (6), 1299–1311. https://doi.org/10.1007/s10950-019-09867-6.

Talebi, M., Zare, M., Noroozinejad Farsangi, E., Soghrat, M.R., Maleki, V., Esmaeili, S., 2021. Development of risk-targeted seismic hazard maps for the Iranian Plateau. Soil Dynam. Earthq. Eng. 141, 106506. https://doi.org/10.1016/j.soildyn.2020.106506.

Uniform Building Code (with International Conference of Building Officials), 1997. International Conference of Building Officials.

Vamvatsikos, D., 2013. Derivation of new SAC/FEMA performance evaluation solutions with second-order hazard approximation. Earthq. Eng. Struct. Dynam. 42 (8), 1171–1188. https://doi.org/10.1002/eqe.2265.